Universal features of the free-energy functional at the freezing transition for repulsive potentials

Anurag Verma and David M. Ford*
Department of Chemical Engineering, University of Massachusetts, Amherst, Massachusetts 01003, USA
(Received 11 February 2011; revised manuscript received 8 April 2011; published 10 May 2011)

The free-energy difference between coexisting solid and liquid phases is studied in the context of classical density functional theory (DFT). A bridge function is used to represent the higher-order ($n > 2$) terms in the perturbative expansion of the excess Helmholtz free energy, and the values of this bridge function within the solid lattice are determined by inversion using literature Monte Carlo simulation results. Four potential models, specifically hard-sphere and inverse twelfth-, sixth-, and fourth-power repulsive, are studied. The face-centered cubic (fcc) solid is considered for the hard-sphere and inverse twelfth- and sixth-power potentials, while the body-centered cubic (bcc) solid is considered for the inverse sixth- and fourth-power potentials. For a given solid structure there is a remarkable similarity among the bridge functions for different potentials that is analogous to the universality in the sum of elementary diagrams, or bridge functions, of liquid-state theory as originally observed by Rosenfeld and Ashcroft [Phys. Rev. A **20**, 1208 (1979)]. In further analogy with liquid-state theory, the bridge functions in the present problem are plotted as functionals of the second-order convolution term in the perturbative expansion. In each case, the plot indicates a unique functionality in the dense regions of the solid near the lattice sites but a scattered and nonunique behavior in the void regions. Interestingly, knowledge of the functional relationship in the unique region near the lattice sites seems to be sufficient to quantitatively model the solid-fluid phase transition. These qualitative observations are true for both fcc and bcc solid phases, although there are some quantitative differences between them. The findings suggest that pursuit of a closure-based DFT of solid-fluid transitions may be profitable.

DOI: 10.1103/PhysRevE.83.051110 PACS number(s): 05.20.Jj, 64.70.dm

I. INTRODUCTION

The prediction of solid-fluid phase equilibrium from an interparticle potential model is an important problem in condensed matter theory [1,2]. Classical density functional theory (DFT) [3] is a useful tool in this regard because of its low computational cost as compared to particle-based simulation. The key ingredient in DFT is an accurate model for the excess Helmholtz free energy as a functional of the density distribution. DFT approaches may be categorized by the approach to constructing the functional. The nonperturbative approaches comprising the weighted and effective liquid theories [4–10] approximate the free energy by mapping the inhomogeneous state onto an effective homogeneous state determined by imposing structural and thermodynamic constraints on the free-energy functionals. The perturbative approaches, on the other hand, employ a truncated series expansion for the free energy in terms of direct correlation functions of the liquid phase. Recently, we proposed [11] the idea of resumming the higher-order ($n > 2$) terms in the perturbative expansion into a bridge function, in analogy with the approach used by Zhou and Ruckenstein [12] for inhomogeneous fluids near interfaces. The purpose of this paper is to study the bridge function for various interaction potentials at their freezing transition and identify further useful analogies with liquid-state theory.

The next section presents key aspects of the theory, especially the role of bridge functions and how they are extracted from literature simulation data. The results and discussion section is split into two parts, with the fcc and bcc solid phases presented sequentially. Finally some conclusions are given.

II. THEORY

Formally the difference in excess Helmholtz free energy F_{ex} between the solid and liquid states may be represented with a functional integration as

$$\beta F^s_{ex}[\rho_s(\mathbf{r})] - \beta F^l_{ex}[\rho_0] = \int d\mathbf{r} \int_{\rho_0}^{\rho_s(\mathbf{r})} \delta\rho(\mathbf{r}) \frac{\delta\beta F_{ex}[\rho]}{\delta\rho(\mathbf{r})}, \quad (1)$$

where $\beta = 1/k_B T$ with k_B the Boltzmann constant and T the coexistence temperature, ρ_0 is the number density of the liquid, and $\rho_s(\mathbf{r})$ is the number density of the coexisting solid phase. The density of the homogeneous liquid is simply a constant. The density of the ordered solid is commonly represented by a sum of isotropic Gaussian functions centered at the lattice points, i.e., $\rho_s(\mathbf{r}) = \frac{1}{\pi^{3/2} l^3} \Sigma_{i=1}^{i=N_s} \exp[-(\mathbf{r} - \mathbf{R}_i)^2/l^2]$ where l is the Gaussian width that serves as an order parameter, N_s is the total number of particles in a fixed volume of the solid phase, and the $\mathbf{R}_i$ are the Bravais lattice vectors, which are determined by the lattice type and the average solid density ρ_s.

The integrand in Eq. (1) is frequently represented more compactly as the negative of a first-order direct correlation function (DCF), i.e., $\frac{\delta\beta F_{ex}[\rho]}{\delta\rho(\mathbf{r})} = -c^{(1)}(\mathbf{r};\rho)$. Furthermore, the starting point for many DFTs is a functional Taylor series expansion of this DCF about the liquid state, as

$$c^{(1)}(\mathbf{r};\rho) = c_0^{(1)}(\rho_0) + \int d\mathbf{r}_2 \int_{\rho_0}^{\rho} \delta\rho(\mathbf{r}_2) c_0^{(2)}(\mathbf{r},\mathbf{r}_2;\rho_0) + \int d\mathbf{r}_2 d\mathbf{r}_3 \int_{\rho_0}^{\rho} \delta\rho(\mathbf{r}_2)\delta\rho(\mathbf{r}_3) c_0^{(3)}(\mathbf{r},\mathbf{r}_2,\mathbf{r}_3;\rho_0) + \cdots. \quad (2)$$

*ford@ecs.umass.edu

The coefficients in this expansion are the DCFs of the liquid phase, as denoted by the subscript 0. The zeroth- and first-order terms are relatively straightforward to compute because $c_0^{(1)}$ is trivially related to the excess chemical potential and $c_0^{(2)}$ may be obtained with high accuracy from Ornstein-Zernike (OZ) liquid-state theory or simulation. However, the rest of the terms involve three-body and higher correlations that are much more challenging to obtain. The idea behind perturbative DFT is to progressively compute these higher-order terms until they become negligible, although previous work on hard spheres has shown that this is not likely to be profitable [13]. We propose to represent the entire summation of these higher-order terms as a bridge function whose characteristics are yet to be determined. Use of $\rho_s(\mathbf{r})$ as the upper limit in the Taylor series of Eq. (2) yields

$$c_s^{(1)}(\mathbf{r};\rho_s) = c_0^{(1)}(\rho_0) + \gamma(\mathbf{r}) + B(\mathbf{r}), \tag{3}$$

where

$$\gamma(\mathbf{r}) = \int d\mathbf{r}_2 c_0^{(2)}(\mathbf{r},\mathbf{r}_2;\rho_0)[\rho_s(\mathbf{r}_2) - \rho_0] \tag{4}$$

and $B(\mathbf{r})$ is the bridge function. Equations (1)–(4) show that this DFT constructs an excess Helmholtz free-energy functional from the liquid-phase properties (excess chemical potential and second-order DCF) and the bridge function. Setting $B(\mathbf{r}) = 0$ recovers the original DFT of Ramakrishnan and Yussouff [14].

There are some analogies between this DFT of solid-fluid equilibrium and the liquid-state theory. The convolution term $\gamma(\mathbf{r})$ is analogous to the indirect correlation function $\tau(r)$ in OZ theory. Similarly $B(\mathbf{r})$ is analogous to the OZ bridge function $b(r)$ that represents the summation of elementary diagrams. In liquid-state theory, specification of the bridge function is referred to as a closure. Sometimes the specification is done directly on the function $b(r)$, as in the modified-hypernetted-chain (MHNC) [15] and variational modified-hypernetted-chain (VMHNC) [16] closures. In other cases b is represented as a functional of the indirect correlation function, as $b[\tau(r)]$, as in the Percus-Yevick (PY), Verlet-modified (VM), and Martynov-Sarkisov (MS) closures [17]. However, with the exception of our previous work on the hard-sphere potential [11], the nature of the closure in the solid-fluid equilibrium has not been explored yet.

The focus of this work is on repulsive interactions of the type $u(r) = \epsilon(\frac{\sigma}{r})^n$ for which simulation data on solid-fluid equilibrium are readily available. Specifically hard spheres ($n = \infty$) and three common soft repulsion models, $n = 12$, 6, and 4, are employed. Literature studies [18] have shown that the stable solid phase is fcc for large n and bcc for small n, with the dividing point being just above $n = 6$. We consider the stable solid phase for each potential, and we also study the metastable fcc phase for $n = 6$. Four pieces of information at coexistence are needed to calculate the bridge function: lattice type, solid density, liquid density, and Gaussian width parameter l, which is related to the root mean square displacement of solid particles about their lattice sites. Table I summarizes the data and sources.

To generate $B(\mathbf{r})$ from these data for a given potential, a pointwise equality of the total chemical potential in the solid and liquid phases is enforced [11]. Denoting the total Helmholtz free energy as $F = F_{id} + F_{ex}$ with $\beta F_{id} = \int d\mathbf{r}\rho(\mathbf{r}) \ln(\frac{\rho(\mathbf{r})\Lambda^3}{e})$, and using the definition of chemical potential $\mu = \frac{\delta F[\rho]}{\delta\rho(\mathbf{r})}$, the equality of the chemical potentials in combination with Eq. (3) yields

$$B(\mathbf{r}) = \ln\left(\frac{\rho_s(\mathbf{r})}{\rho_0}\right) - \gamma(\mathbf{r}). \tag{5}$$

This is the key equation for extracting $B(\mathbf{r})$ from the simulation data given in Table I. The solid density $\rho_s(\mathbf{r})$ is modeled with the sum of Gaussian functions described above, using the lattice type, ρ_s, and l. The value of $\gamma(\mathbf{r})$ as defined in Eq. (4) is evaluated using the liquid-state DCF from a highly accurate VMHNC calculation at the density ρ_0. Since $\gamma(\mathbf{r})$ and $\rho_s(\mathbf{r})$ are periodic in the three-dimensional solid lattice, these quantities were evaluated in the smallest repetitive unit cell of the solid.

TABLE I. Coexistence data for repulsive potentials. For the soft potentials $\beta\epsilon = 10$.

n	ρ_s	ρ_0	l	Structure	Ref.
∞	1.0409	0.9435	0.1139	fcc	[19]
12	0.6804	0.6557	0.1459	fcc	[20]
6	0.7494	0.7399	0.1513	fcc	[20]
6	0.7339	0.7247	0.1876	bcc	[20]
4	1.0225	1.0185	0.1591	bcc	[20]

III. RESULTS AND DISCUSSION

A. fcc lattice structure

Plots of $B(\mathbf{r})$ for two different two-dimensional slices through the tetrahedral unit cell of the fcc lattice are shown in Fig. 1, for the $n = \infty$, 12, and 6 potentials. The most striking feature of this figure is that $B(\mathbf{r})$ is qualitatively similar across the three potentials. The results for the bottom plane show that higher (less negative) values are found at the lattice sites, which even become slightly positive for the hard spheres, while lower (more negative) values are found in the voids. The results for the middle section show relatively lower values of B because of the larger amounts of void space, but with high values seen in the corners because of their proximity to the lattice sites above and below.

The qualitative similarity of $B(\mathbf{r})$ across the three potentials is reminiscent of observations by Rosenfeld and Ashcroft on the bridge function of liquid-state theory [15]. They observed that $b(r)$ had roughly the same shape across a wide range of interaction potentials and thermodynamic conditions (density, temperature) and was thus deemed to "constitute the same universal family of curves." Remarkably, an analogous universality also appears to hold for $B(\mathbf{r})$ at solid-fluid equilibrium for an fcc lattice, at least for the three repulsive potentials studied here. Rosenfeld and Ashcroft [15,16] and Lado *et al.* [21] were able to exploit the universality of $b(r)$ in a quantitative way by using known bridge functions for hard spheres at different packing fractions $b_{HS}(r;\eta)$ as reference data. For any interaction potential, one could employ $b(r) \approx b_{HS}(r;\eta^*)$ with the effective packing fraction η^* chosen

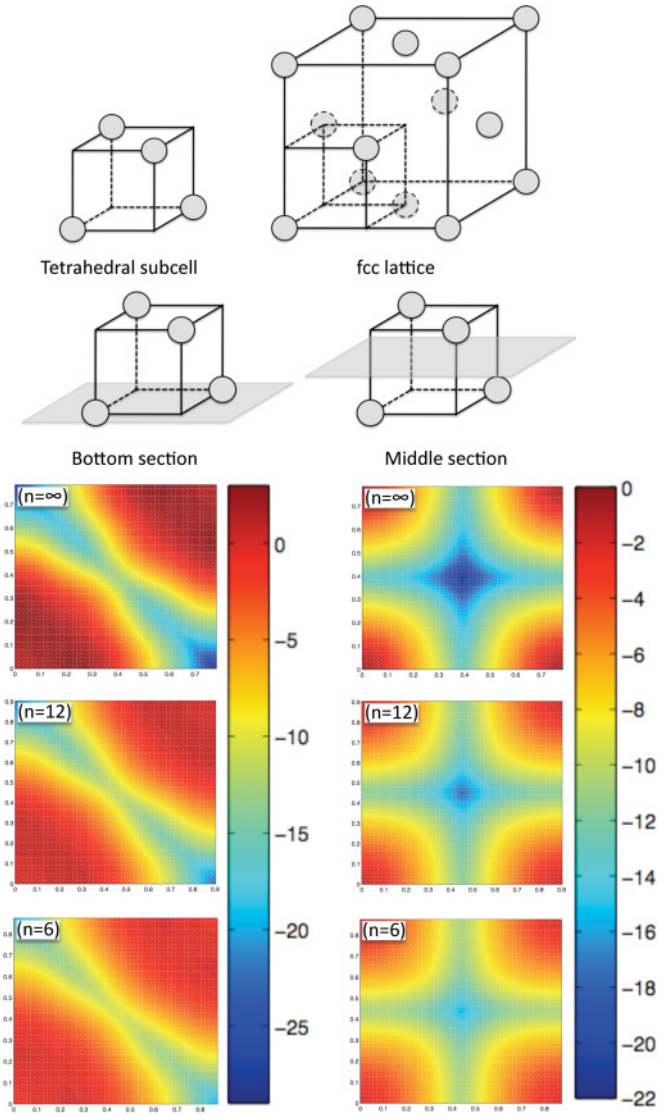

FIG. 1. (Color online) Location of the subcell of interest in the fcc lattice (top). Plots of the values of $B(\mathbf{r})$ in planar slices along the bottom (left column) and middle (right column) of the unit cell. A plot of the top plane would just be a 90° rotation of that for the bottom plane.

to satisfy thermodynamic consistency or minimize the free energy, under the conditions of interest. The VMHNC closure of this type is among the most accurate in predicting liquid structure. However, it is difficult to extend this approach to the present problem of solid-fluid equilibrium. Since solid-fluid coexistence for hard spheres occurs at one thermodynamic state point, there is no natural parametric set of hard-sphere bridge functions $\{B_{HS}(\mathbf{r})\}$ to employ. Furthermore, even if such a set were available, there are no *a priori* thermodynamic consistency criteria that could be applied in choosing the best one.

As mentioned above, another common approach to the bridge function in liquid-state theory is to represent it as a functional of the indirect correlation function, so that $b = b[\tau(r)]$. The analogy for solid-fluid equilibrium is $B = B[\gamma(\mathbf{r})]$. Equation (5) can be readily used to generate a parametric plot of $B[\gamma]$ with data points taken throughout

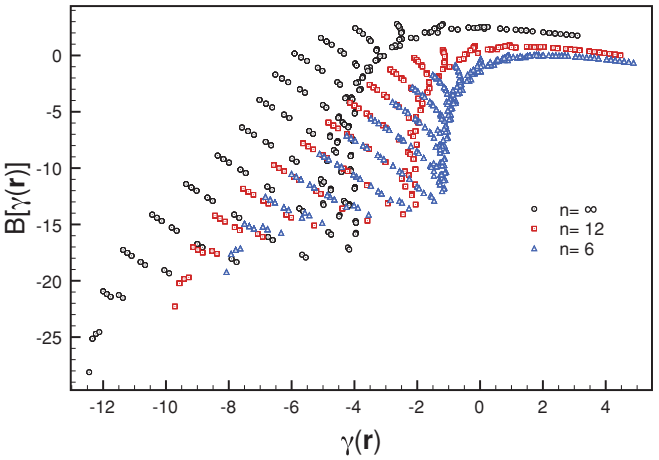

FIG. 2. (Color online) Parametric plots of $B[\gamma]$ for three different interaction potentials with an fcc solid.

the subcell, as seen in Fig. 2. A figure of this type is often called a Duh-Haymet plot in liquid-state theory. Presenting the data in this form again illustrates the qualitative similarity in the bridge functions across the three different potentials. For each potential there is a region of unique $B[\gamma]$ functionality at high values of γ but large scatter and nonuniqueness at lower values of γ. Further insight can be gained by creating a parametric plot of $\gamma(\mathbf{r})$ with respect to $\rho_s(\mathbf{r})/\rho_0$ as seen in Fig. 3. Now it is clear that high values of $\gamma(\mathbf{r})$ correspond to regions of high density in the lattice, which occur in the vicinity of lattice sites (particle cores). Looking back at Fig. 2 we conclude that for each potential there is a unique $B[\gamma]$ functionality in high-density regions near the lattice sites but no such functionality in the void regions. This observation also has an analogy in liquid-state theory, where Duh-Haymet plots show unique $b[\tau]$ functionality near the particle core (at the first peak region) but scatter outside [22].

Figure 2 begs the question of whether some analytical form of $B[\gamma]$ would suffice as a closure. For each interaction potential, we proposed the simple quadratic form $B[\gamma] = a\gamma^2 + b\gamma + c$. The values of the coefficients were determined

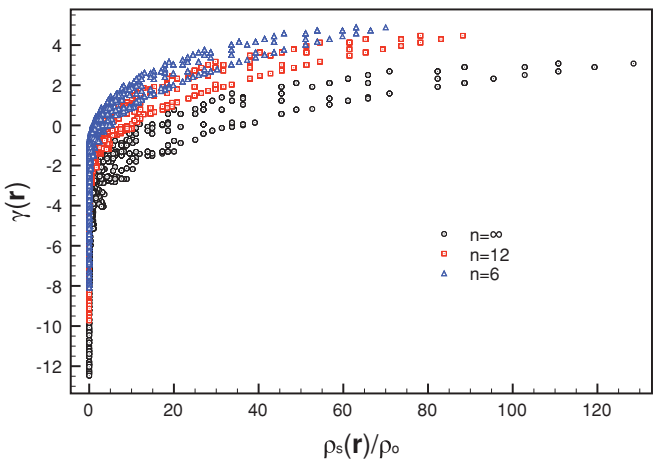

FIG. 3. (Color online) Plot showing γ vs $\rho_s(1)/\rho_0$ for the three potentials with an fcc solid. Note that high values of γ occur at high density ratio which happens at the lattice sites.

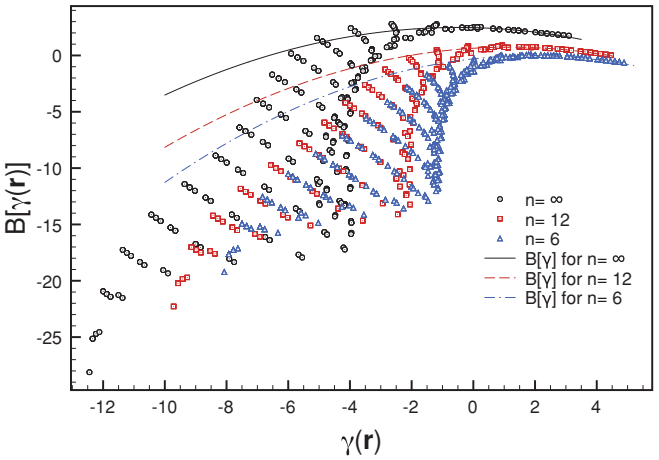

FIG. 4. (Color online) $B[\gamma]$ for $n = \infty$ $\{B[\gamma] = -0.0665\gamma^2 - 0.0663\gamma + 2.4689\}$, $n = 12$ $\{B[\gamma] = -0.0712\gamma^2 + 0.1669\gamma + 0.6385\}$ and $n = 6$ $\{B[\gamma] = -0.0796\gamma^2 + 0.3005\gamma - 0.3024\}$.

by iteratively solving the solid-fluid coexistence problem using the DFT model in Eqs. (1)–(4) until a set of values $\{a,b,c\}$ that satisfied the known properties (Table I) was found; details of

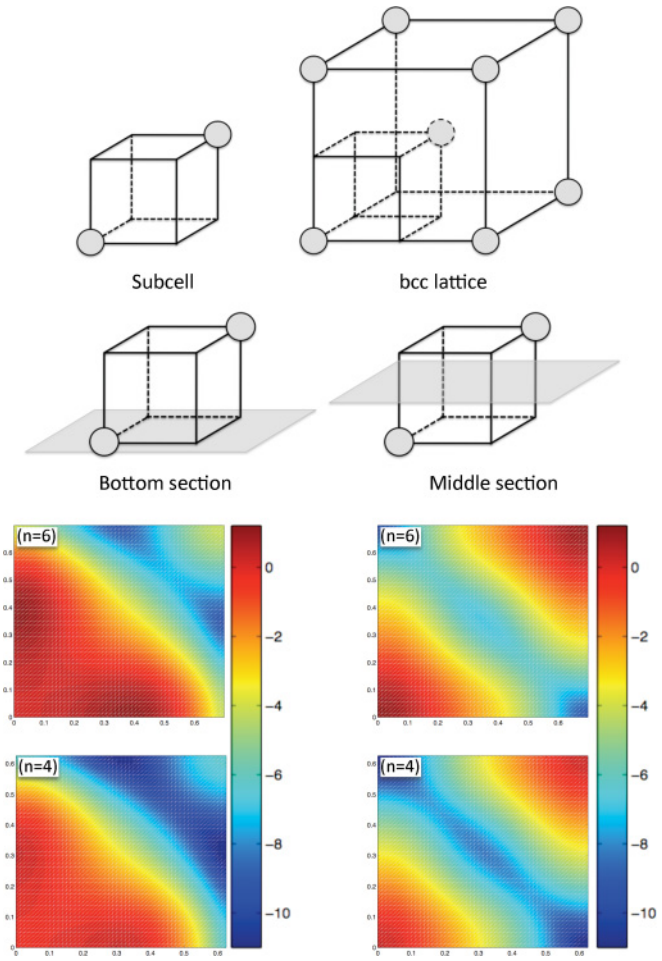

FIG. 5. (Color online) Location of the subcell of interest in the bcc lattice (top). Plots of the values of $B(\mathbf{r})$ in planar slices along the bottom (left column) and middle (right column) of the unit cell. A plot of the top plane would just be a 90° rotation of that for the bottom plane.

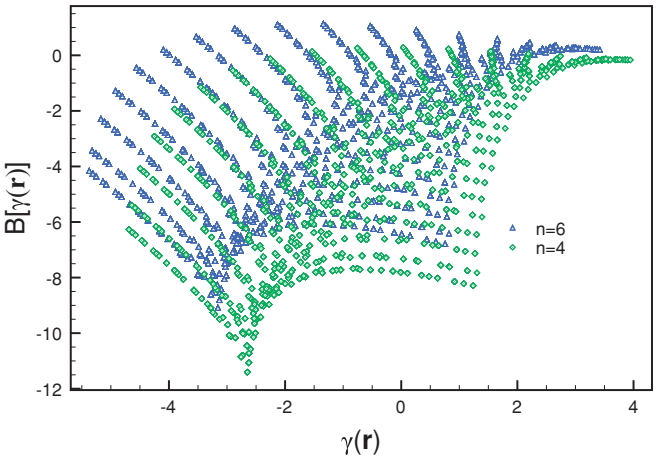

FIG. 6. (Color online) Parametric plot of B vs $\gamma(\mathbf{r})$ for two different interaction potentials with a bcc solid.

this calculation are given in our previous publication [11]. Figure 4 shows the quadratic polynomials thus obtained and how they compare to the parametric data. Strikingly, each polynomial matches its corresponding parametric plot at high values of γ, where there is a unique functionality in the parametric data, but not in the low-γ scattered region. Thus the thermodynamic properties at the phase transition appear to be governed by the behavior of the bridge function in the high-density regions of the solid lattice and rather insensitive to its behavior elsewhere. This observation also has an analogy in liquid-state theory, where the behavior of the bridge function at particle-particle separations close to the location of the first peak in the radial distribution function has the greatest impact on the thermodynamic properties [15], and the behavior inside the core is largely irrelevant [21].

B. bcc lattice structure

A similar analysis was carried out for the bcc solid-fluid equilibrium for the $n = 6$ and 4 potentials. The plots of $B(\mathbf{r})$ for different slices through the unit cell are shown in Fig. 5. There is clearly a similarity in the bridge functions of these two potentials. However, these plots are qualitatively different from those for the fcc solids in Fig. 1 because of the differences in lattice geometry. While high values of $B(\mathbf{r})$ still occur in the vicinity of a lattice site, now the highest values occur slightly off center, forming a split peak arrangement.

The parametric $B[\gamma]$ plots in Fig. 6 also indicate that the bridge functions of the bcc solids have a slightly different character from those of the fcc solids. The bcc plots show two distinct sets of branches (as compared to one set for fcc) within their envelope, causing them to appear wider (although they actually span a smaller range of γ). We investigated in more depth how the different regions of the lattice contributed to the parametric plot. The points lying along the top left boundary of the envelope are obtained by moving along a particle-containing edge of the subcell (as shown in Fig. 5) of the bcc lattice, while the points along the bottom right boundary are obtained by moving along a line joining two lattice sites (i.e., a Bravais lattice vector). We observed the same to be true for the fcc case as well. Therefore the different

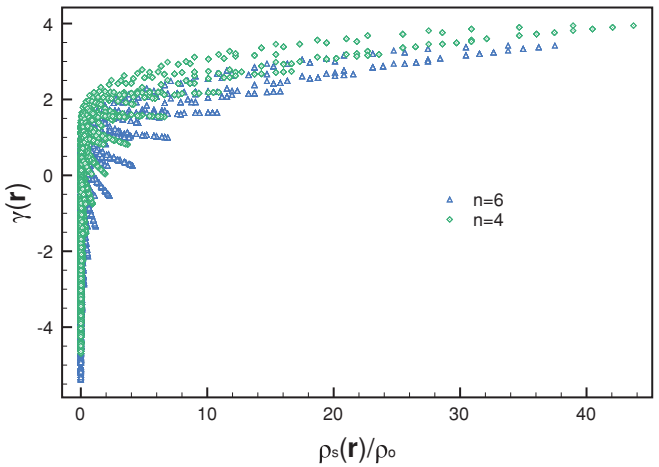

FIG. 7. (Color online) Plot of γ vs $\rho_s(\mathbf{r})/\rho_o$ for the two potentials with a bcc solid.

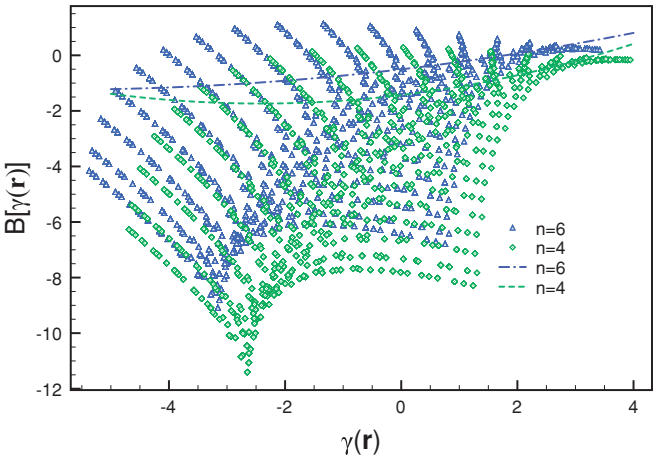

FIG. 8. (Color online) $B[\gamma]$ for $n = 6$ $\{B[\gamma] = 0.0206\gamma^2 + 0.2454\gamma - 0.5045\}$ and $n = 4$ $\{B[\gamma] = 0.0522\gamma^2 + 0.2524\gamma - 1.4305\}$.

character of the bcc and fcc parametric plots is a reflection of the different lattice geometries.

Figure 7 shows that high values of γ occur at the high-density regions in the bcc lattice, so that the sharp region at high γ in Fig. 6 corresponds to the sites in the bcc lattice, analogous to our observations for the fcc structure. As in the case of the fcc solids, quadratic polynomials were found that exactly reproduced the solid-fluid coexistence properties given in Table I. As seen in Fig. 8, these polynomials pass through most of the unique functionlike region of the parametric data at the largest γ, but they are concave up and follow the data in a tangential fashion, in contrast to the direct overlap seen in Fig. 4 for the fcc case.

IV. CONCLUSION

We have constructed a DFT of the solid-fluid transition wherein the higher-order terms in the perturbative excess free-energy expansion are represented with a bridge function. We have empirically calculated this bridge function for four different repulsive potentials, and two different lattice types, by inverting their known coexistence properties as determined by simulation. For a given solid lattice structure (fcc or bcc), the bridge functions for different potentials, whether observed directly as $B(\mathbf{r})$ or parametrically as $B[\gamma(\mathbf{r})]$, show a similarity in shape that is reminiscent of the universality observed for the bridge functions b of liquid-state theory. There are significant differences between the bridge functions found for the two different solid structures, however. On a practical note, quadratic representations of $B[\gamma]$ that exactly reproduce the known solid-fluid coexistence properties were found for each potential. Although these closures are purely empirical in nature, the nature of the findings suggests that more fundamental methods of closure development would be worth pursuing. In particular, analysis of $B[\rho]$ using the formalism of graph theory [17] might generate useful approximate closures. A successful development program along these lines would lead to a situation like the current one in liquid-state theory, where reasonably accurate thermodynamic property predictions may be made across a wide variety of potential interactions by choosing judiciously from a small set of closures.

ACKNOWLEDGMENTS

Acknowledgment is made to the Donors of the American Chemical Society Petroleum Research Fund for partial support of this research. This material is based upon work supported by the National Science Foundation under Grant No. 0835532.

[1] P. A. Monson and D. A. Kofke, Adv. Chem. Phys. **115**, 113 (2000).
[2] P. A. Monson, AIChE J. **54**, 1122 (2008).
[3] *Fundamentals of Inhomogeneous Fluids*, edited by D. Henderson (Marcel-Dekker, New York, 1992).
[4] P. Tarazona, Mol. Phys. **52**, 81 (1984).
[5] P. Tarazona, Phys. Rev. A **31**, 2672 (1985).
[6] W. A. Curtin and N. W. Ashcroft, Phys. Rev. A **32**, 2909 (1985).
[7] A. R. Denton and N. W. Ashcroft, Phys. Rev. A **39**, 4701 (1989).
[8] M. Baus and J. L. Colot, Mol. Phys. **55**, 653 (1985).
[9] M. Baus, J. Phys.: Condens. Matter **1**, 3131 (1989).
[10] J. F. Lutsko and M. Baus, Phys. Rev. A **41**, 6647 (1990).
[11] A. Verma and D. M. Ford, Phys. Rev. E **80**, 031109 (2009).
[12] S. Zhou and E. Ruckenstein, J. Chem. Phys. **112**, 8079 (2000).
[13] W. A. Curtin, J. Chem. Phys. **88**, 7050 (1988).
[14] T. V. Ramakrishnan and M. Yussouff, Phys. Rev. B **19**, 2775 (1979).
[15] Y. Rosenfeld and N. W. Ashcroft, Phys. Rev. A **20**, 1208 (1979).
[16] Y. Rosenfeld, J. Stat. Phys. **42**, 437 (1986).

[17] J. P. Hansen and I. R. McDonald, *Theory of Simple Liquids* (Harcourt Brace and Company, 1996).
[18] R. Agrawal and D. A. Kofke, Phys. Rev. Lett. **74**, 122 (1995).
[19] W. G. Hoover and F. H. Ree, J. Chem. Phys. **49**, 3609 (1968).
[20] A. Kol and B. B. Laird, Mol. Phys. **90**, 951 (1997).
[21] F. Lado, S. M. Foiles, and N. W. Ashcroft, Phys. Rev. A **28**, 2374 (1983).
[22] R. Fantoni and G. Pastore, J. Chem. Phys. **120**, 10681 (2004).